Chapter 4

Two interfacial collinear Griffith cracks in thermo-elastic composite media

4.1 Introduction

In many engineering disciplines viz., electronics, aerospace and nuclear energy, lot of research has already been done during the study of the behavior of stress and displacement fields at the vicinity of the crack tip situated at the interface of the composite materials subject to thermal loading. Orthotropic composite materials are widely used in structural materials due to their light weight and strong in nature. When a cracked orthotropic composite material is used in high or low temperature region, then heat flows through material. In this case it is important to determine the thermal stress intensity around the crack, which occurs due to the disturbance in heat flux. The investigation of thermo-elastic field and thermal stress concentration around the crack help to understand the stability and life of the cracked engineering materials and structures. According to linear elastic fracture mechanics stress at the vicinity of the crack tip is singular. It is directly proportional to the inverse of square root of distance from the crack tip. Many observations of thermo-elastic cracked surfaces show that the thermal stress singularity at the vicinity of the crack tips are same as those with mechanical stresses. But the nature of singularity becomes different for an interfacial crack. The occurrence of the interfacial cracks at the surface of structural components

---

The contents of this chapter have been accepted for publication in **Thermal Science.**

due to thermal and mechanical loading becomes an important research topic in fracture mechanics. For analyzing interfacial cracks, many studies were conducted under thermal steady state condition for orthotropic composite materials.

Sih (1962) determined the stress intensity factor of a crack in an infinite plate when heat flows perpendicular to the crack surface. Later, Sekine (1977) determined the stress intensity factor of a crack due to heat flux. The thermal stresses in an infinite plate due to heat flux for two cracks have been determined by the same author. Stress intensity factors around two collinear cracks were evaluated by Chen and Zhang (1988) in an orthotropic plate under heat flux. Thermal stress for a single crack in an infinite elastic layer and thermal stress around two parallel cracks had been determined by Itou and Rengen ((1993, 1995)). Chen and Zhang (1993) have determined the thermal stress in an orthotropic strip containing two collinear cracks. Itou (2001) evaluated stress intensity factors for two parallel cracks in an infinite orthotropic plate due to heat flux. Baksi et al. (2007) have solved the problem of determining the thermal stresses and displacement fields in an orthotropic plane containing a pair of equal collinear Griffith cracks using integral transform technique based upon displacement potential under steady state temperature field. Zhong et al. (2013) examined the behavior of two collinear cracks embedded in an orthotropic solid using Fourier integral transform technique, under uniform heat flux and mechanical loading on the cracked surfaces. Problem related to thermal stress and strain can also be found in the research chapters (Thakur (2014a, 2014b), Zhu et al. (2014), Sills and Dolev (2004), Itou (2000), De and Patra (1992) and Itou (1993)).

In the present chapter an endeavour has been taken to determine the stress intensity factors at the tips of a pair of collinear Griffith cracks situated at the interface of two orthotropic thermo-elastic half planes subject to uniform heat flux and also to determine the energy required for creating two new surfaces and plastic deformation of the cracks under steady-state temperature field. The problem has been reduced to a pair of second kind Fredholm integral equations, which are solved numerically using Jacobi polynomials. Numerical values of the stress intensity factors at the tips of the cracks for different prescribed crack lengths are presented through graphs for different particular cases. Numerical values of other physical quantity crack energy obtained through different forms of the displacement potential functions are also presented graphically.

4.2 Problem Formulation

Let us consider a mathematical model of two bonded homogeneous orthotropic elastic half planes $0 \le y < \infty$ and $-\infty < y \le 0$ containing a pair of collinear Griffith cracks situated symmetrically at the interface $y = 0$ when Cartesian co-ordinate axes coincide with the axes of symmetry of the elastic material. When thermal conditions are applied to the surface of an arbitrary two dimensional orthotropic half planes, the temperature field only depends upon in- plane co-ordinates under steady state condition. The temperature distribution functions $T^{(i)}(x, y)$ are assumed to satisfy the following heat conduction equation in the orthotropic media.

$$\frac{\partial^2 T^{(i)}}{\partial x^2} + K^{(i)^2} \frac{\partial^2 T^{(i)}}{\partial y^2} = 0, \tag{4.1}$$

where $(K^{(i)})^2 = K_y^{(i)} / K_x^{(i)}$ and $K_y^{(i)}$, $K_x^{(i)}$ $(i = 1, 2)$ are the thermal conductive coefficients along y and x directions respectively for each half plane. The general solution of $T^{(j)}(x, y)$ is (Akoz and Tauchert (1972))

$$T^{(j)}(x, y) = \tfrac{1}{2\pi} \int_0^\infty \{A^{(j)}(p) \exp[p(ix - y / K^{(j)})] + \overline{A}^{(j)}(p) \exp[p(-ix - y / K^{(j)})]\} dp, \tag{4.2}$$

where $i=\sqrt{-1}$, $j=1,2$ and $A^{(j)}(p)$ and $\overline{A}^{(j)}(p)$ are the arbitrary functions of p.

Here we have assumed that

$$T^{(i)}(x,0)=h^{(i)}(x) \tag{4.3}$$

and hence the Fourier integral form of temperature distribution may be written as

$$T^{(i)}(x,0)=\tfrac{1}{2\pi}\int_{0}^{\infty}\{\int_{-\infty}^{\infty}h^{(i)}(\xi)\exp[p(i\xi)]\exp[p(ix)]+h^{(i)}(\xi)\exp[p(i\xi)]\exp[p(-ix)]d\xi\}\,dp. \tag{4.4}$$

From equations (4.2) and (4.4), we get

$$A^{(i)}(p)=\int_{-\infty}^{\infty}h^{(i)}(\xi)\exp[-ip\xi]\,d\xi,\ \overline{A}^{(i)}(p)=\int_{-\infty}^{\infty}h^{(i)}(\xi)\exp[ip\xi]\,d\xi. \tag{4.5}$$

From equations (4.2) and (4.5), the temperature distribution $T^{(i)}(x,y)$ is obtained as

$$T^{(i)}(x,y)=\frac{1}{\pi}\int_{-\infty}^{\infty}\tfrac{(y/K^{(i)})h^{(i)}(\xi)d\xi}{(y/K^{(i)})^2+(\xi-x)^2}. \tag{4.6}$$

If we consider $h^{(i)}(x)=\delta(x)$, (4.7)

where *h(x)* is the prescribed temperature distribution become line source along *y*-axis and $\delta(x)$ is Dirac delta function, the resultant temperature distribution is obtained as

$$T^{(i)}(x,y)=\frac{1}{\pi}\frac{(y/K^{(i)})}{(y/K^{(i)})^2+x^2}. \tag{4.8}$$

The relations between plane stress induced by the distribution of temperature and displacement components $u^{(i)}(x,y)$ and $v^{(i)}(x,y)$ along *x* and *y* directions are given by

$$\sigma_{xx}^{(i)}(x,y)=C_{11}^{(i)}\frac{\partial u^{(i)}}{\partial x}+C_{12}^{(i)}\frac{\partial v^{(i)}}{\partial y}-\beta_x^{(i)}T^{(i)}, \tag{4.9}$$

$$\sigma_{yy}^{(i)}(x,y)=C_{12}^{(i)}\frac{\partial u^{(i)}}{\partial x}+C_{22}^{(i)}\frac{\partial v^{(i)}}{\partial y}-\beta_y^{(i)}T^{(i)}, \tag{4.10}$$

$$\sigma_{xy}^{(i)}(x,y)=C_{66}^{(i)}(\frac{\partial u^{(i)}}{\partial x}+\frac{\partial v^{(i)}}{\partial y}), \tag{4.11}$$

The elastic constants are given by $C_{11}^{(i)}=\frac{E_{xx}^{(i)}}{1-\upsilon_{xy}^{(i)}\,\upsilon_{yx}^{(i)}}$, $C_{22}^{(i)}=\frac{E_{yy}^{(i)}}{1-\upsilon_{xy}^{(i)}\,\upsilon_{yx}^{(i)}}$, $C_{12}^{(i)}=\frac{E_{yy}^{(i)}\upsilon_{xy}^{(i)}}{1-\upsilon_{xy}^{(i)}\,\upsilon_{yx}^{(i)}}=\frac{E_{xx}^{(i)}\upsilon_{yx}^{(i)}}{1-\upsilon_{xy}^{(i)}\,\upsilon_{yx}^{(i)}}$, $C_{66}^{(i)}=G_{xy}^{(i)}$ and stress – temperature coefficients are defined by $\beta_x^{(i)}=C_{12}^{(i)}\,\alpha_{yy}^{(i)}+C_{11}^{(i)}\,\alpha_{xx}^{(i)}$, $\beta_y^{(i)}=C_{12}^{(i)}\,\alpha_{xx}^{(i)}+C_{22}^{(i)}\,\alpha_{yy}^{(i)}$, where $E_{xx}^{(i)}$, $E_{yy}^{(i)}$ are the Young's moduli, $G_{xy}^{(i)}$ is shear modulus, $\upsilon_{xy}^{(i)}$ and $\upsilon_{yx}^{(i)}$ are Poisson's ratios, $\alpha_{xx}^{(i)}$ and $\alpha_{yy}^{(i)}$ are linear expansion coefficients. The quantities with superscripts $i=1,2$ refer to those for the half plane-1 and half plane-2 respectively. It is to be noted that the unit of $C_{jk}^{(i)}$'s is taken in *GPa* and units of $\beta_x^{(i)}$ and $\beta_y^{(i)}$ are considered as *GPa/deg*.

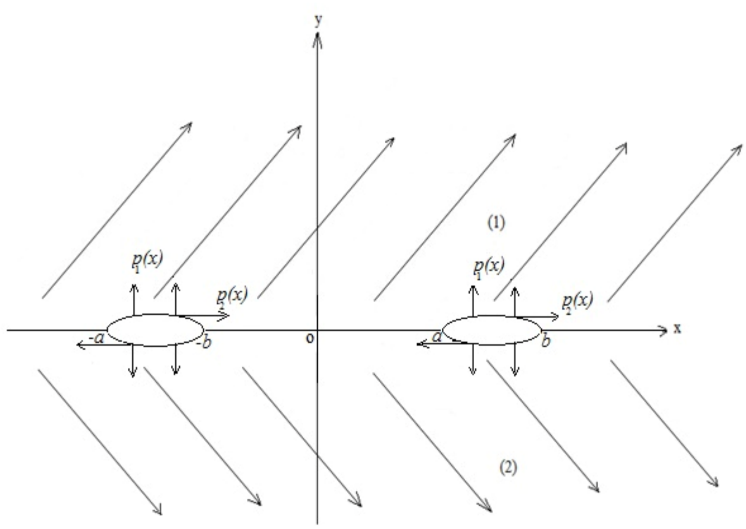

Fig. 4.1 Geometry of the Problem

The displacement equations of equilibrium are given by

$$C_{11}^{(i)}\frac{\partial^2 u^{(i)}}{\partial x^2}+C_{66}^{(i)}\frac{\partial^2 u^{(i)}}{\partial y^2}+(C_{12}^{(i)}+C_{66}^{(i)})\frac{\partial^2 v^{(i)}}{\partial x\partial y}=\beta_x^{(i)}\frac{\partial T^{(i)}}{\partial x}, \tag{4.12}$$

$$C_{22}^{(i)}\frac{\partial^2 v^{(i)}}{\partial y^2}+C_{66}^{(i)}\frac{\partial^2 v^{(i)}}{\partial x^2}+(C_{12}^{(i)}+C_{66}^{(i)})\frac{\partial^2 u^{(i)}}{\partial x\partial y}=\beta_y^{(i)}\frac{\partial T^{(i)}}{\partial y}. \tag{4.13}$$

The quantities with superscripts $i=1,2$ refer to those for the half plane-1 and half plane-2 respectively. It is assumed that at the interface $y=0$, the cracks defined by $a<|x|<b$ are opened by internal normal and shearing tractions $p_1(x)$ and $p_2(x)$ respectively (Fig. 4.1). For the described problem the boundary conditions on $y=0$ are given by

$$\sigma_{yy}^{(1)}(x,0)=-p_1(x), \qquad a\le|x|\le b, \tag{4.14}$$

$$\sigma_{xy}^{(1)}(x,0)=-p_2(x), \qquad a\le|x|\le b, \tag{4.15}$$

$$u^{(1)}(x,0)=u^{(2)}(x,0), \qquad |x|<a\,,\ |x|>b, \tag{4.16}$$

$$v^{(1)}(x,0)=v^{(2)}(x,0), \qquad |x|<a\,,\ |x|>b, \tag{4.17}$$

$$\sigma_{yy}^{(1)}(x,0)=\sigma_{yy}^{(2)}(x,0), \qquad -\infty<x<\infty, \tag{4.18}$$

$$\sigma_{xy}^{(1)}(x,0)=\sigma_{xy}^{(2)}(x,0), \qquad -\infty<x<\infty. \tag{4.19}$$

4.3 Solution of the problem

During solution of the problem, we first introduce displacement potentials $\psi^{(i)}(x,y)$ and $\phi_j^{(i)}(x,y)$ (Sharma (1958)) as

$$\psi^{(i)}(x,y)=\frac{1}{2\pi}\int_0^\infty\{A^{(i)}(p)B^{(i)}(p)e^{p\{ix-(y/K)\}}+\overline{A}^{(i)}(p)\overline{B}^{(i)}(p)e^{p\{-ix-(y/K)\}}\}\,dp. \tag{4.20}$$

Potential functions for the half planes are given by

$$\phi_1^{(i)}(x,y)=\frac{2}{\pi}\int_0^\infty s^{-2}A_1^{(i)}(s)e^{-\frac{sy}{\sqrt{\mu_1^{(i)}}}}\cos(sx)\,ds \tag{4.21}$$

$$\phi_2^{(i)}(x,y)=\frac{2}{\pi}\int_0^\infty s^{-2}A_2^{(i)}(s)e^{-\frac{sy}{\sqrt{\mu_2^{(i)}}}}\cos(sx)\,ds\,,\quad i=1,2. \tag{4.22}$$

The displacement components $u^{(i)}(x,y)$ and $v^{(i)}(x,y)$ are written as

$$u^{(i)}=\frac{\partial\psi^{(i)}}{\partial x}+\frac{\partial\phi_1^{(i)}}{\partial x}+\frac{\partial\phi_2^{(i)}}{\partial x}\ \text{ and }\ v^{(i)}=\mu_1^{(i)}\frac{\partial\psi^{(i)}}{\partial y}+k_1^{(i)}\frac{\partial\phi_1^{(i)}}{\partial y}+k_2^{(i)}\frac{\partial\phi_2^{(i)}}{\partial y}. \tag{4.23}$$

The corresponding thermal stresses are

$$\frac{\sigma_{xx}^{(i)}(x,y)}{C_{66}^{(i)}}=-\left[(1+k_1^{(i)})\frac{\partial^2\phi_1^{(i)}}{\partial y^2}+(1+k_2^{(i)})\frac{\partial^2\phi_2^{(i)}}{\partial y^2}+(1+\eta^{(i)})\frac{\partial^2\psi^{(i)}}{\partial y^2}\right], \tag{4.24}$$

$$\frac{\sigma_{yy}^{(i)}(x,y)}{C_{66}^{(i)}}=\left[(1+k_1^{(i)})\mu_1^{(i)}\frac{\partial^2\phi_1^{(i)}}{\partial y^2}+(1+k_2^{(i)})\mu_2^{(i)}\frac{\partial^2\phi_2^{(i)}}{\partial y^2}-(1+\eta^{(i)})\frac{\partial^2\psi^{(i)}}{\partial x^2}\right], \tag{4.25}$$

$$\frac{\sigma_{xy}^{(i)}(x,y)}{C_{66}^{(i)}}=\left[(1+k_1^{(i)})\frac{\partial^2\phi_1^{(i)}}{\partial x\partial y}+(1+k_2^{(i)})\frac{\partial^2\phi_2^{(i)}}{\partial x\partial y}+(1+\eta^{(i)})\frac{\partial^2\psi^{(i)}}{\partial x\partial y}\right]. \tag{4.26}$$

The displacement equations (4.12)-(4.13) are satisfied by equation (4.20) for non trivial $\phi_j^{(i)}(x,\ y)$ if

$$\eta^{(i)}=\frac{\beta_y^{(i)}(C_{66}^{(i)}-K^{(i)2}C_{11}^{(i)})+\beta_x^{(i)}(C_{12}^{(i)}+C_{66}^{(i)})K^{(i)2}}{\beta_x^{(i)}(C_{22}^{(i)}-K^{(i)2}C_{66}^{(i)})-\beta_y^{(i)}(C_{12}^{(i)}+C_{66}^{(i)})}, \tag{4.27}$$

$$p^2B=p^2\overline{B}=K^{(i)2}\,\frac{\beta_x^{(i)}(C_{22}^{(i)}-K^{(i)2}C_{66}^{(i)})-\beta_y^{(i)}(C_{12}^{(i)}+C_{66}^{(i)})}{(C_{22}^{(i)}-K^{(i)2}C_{66})(C_{66}^{(i)}-K^{(i)2}C_{11})+K^{(i)}(C_{12}^{(i)}+C_{66}^{(i)})^2}=k^{(i)}. \tag{4.28}$$

Here potential functions $\phi_j^{(i)}(x,y)$ satisfy the following differential equations

$$\left(\frac{\partial^2}{\partial x^2}+\frac{\partial^2}{\partial y^2}\right)\phi_j^{(i)}(x,y)=0,\ i=1,2\ ;\ j=1,2,$$

where $\mu_1^{(i)}$ and $\mu_2^{(i)}$ are the real roots of the equation

$$C_{11}^{(i)}C_{66}^{(i)}\mu^{(i)2}+[(C_{12}^{(i)})^2+2C_{12}^{(i)}C_{66}^{(i)}-C_{11}^{(i)}C_{22}^{(i)}]\mu^{(i)}+C_{212}^{(i)}C_{66}^{(i)}=0, \tag{4.29}$$

with $k_j^{(i)} = \dfrac{C_{11}^{(i)}\mu_j^{(i)} - C_{66}^{(i)}}{C_{66}^{(i)} + C_{12}^{(i)}}$. (4.30)

$A_1^{(i)}(s)$ and $A_2^{(i)}(s)$ $(i=1,2)$ are the undetermined functions. Applying the boundary conditions (4.18) and (4.19), we get

$$A_1^{(2)}(s) = \frac{k^{(2)}(1+\eta^{(2)})\sqrt{\mu_1^{(2)}}}{2(\sqrt{\mu_2^{(2)}}-\sqrt{\mu_1^{(2)}})(1+k_1^{(2)})}\left(\frac{\sqrt{\mu_2^{(2)}}}{K^{(2)}}\right) + \frac{C_{66}^{(1)}}{C_{66}^{(2)}}\frac{k^{(1)}(1+\eta^{(1)})}{2K^{(1)}}\frac{\sqrt{\mu_1^{(2)}}(\sqrt{\mu_{22}^{(2)}}-K^{(1)})}{(1+k_1^{(2)})(\sqrt{\mu_2^{(2)}}-\sqrt{\mu_1^{(2)}})}$$

$$+ A_1^{(1)}(s)\frac{\sqrt{\mu_1^{(2)}}(1+k_1^{(1)})(\sqrt{\mu_2^{(2)}}-\sqrt{\mu_1^{(1)}})}{\sqrt{\mu_1^{(1)}}(1+k_1^{(2)})(\sqrt{\mu_2^{(2)}}-\sqrt{\mu_1^{(2)}})} + A_2^{(1)}(s)\frac{\sqrt{\mu_1^{(2)}}(1+k_2^{(1)})(\sqrt{\mu_2^{(2)}}-\sqrt{\mu_2^{(1)}})}{\sqrt{\mu_2^{(1)}}(1+k_1^{(2)})(\sqrt{\mu_2^{(2)}}-\sqrt{\mu_1^{(2)}})},$$

$$A_2^{(2)}(s) = \frac{k^{(2)}(1+\eta^{(2)})\sqrt{\mu_2^{(2)}}}{2(\sqrt{\mu_1^{(2)}}-\sqrt{\mu_2^{(2)}})(1+k_2^{(2)})}\left(\frac{\sqrt{\mu_1^{(2)}}}{K^{(2)}}\right) + \frac{C_{66}^{(1)}}{C_{66}^{(2)}}\frac{k^{(1)}(1+\eta^{(1)})}{2K^{(1)}}\frac{\sqrt{\mu_2^{(2)}}(\sqrt{\mu_{21}^{(2)}}-K^{(1)})}{(1+k_2^{(2)})(\sqrt{\mu_1^{(2)}}-\sqrt{\mu_2^{(2)}})}$$

$$+ A_1^{(1)}(s)\frac{\sqrt{\mu_2^{(2)}}(1+k_1^{(1)})(\sqrt{\mu_1^{(2)}}-\sqrt{\mu_1^{(1)}})}{\sqrt{\mu_1^{(1)}}(1+k_2^{(2)})(\sqrt{\mu_1^{(2)}}-\sqrt{\mu_2^{(2)}})} + A_2^{(1)}(s)\frac{\sqrt{\mu_2^{(2)}}(1+k_2^{(1)})(\sqrt{\mu_1^{(2)}}-\sqrt{\mu_2^{(1)}})}{\sqrt{\mu_2^{(1)}}(1+k_2^{(2)})(\sqrt{\mu_1^{(2)}}-\sqrt{\mu_2^{(2)}})}.$$

Boundary conditions (4.16) and (4.17) with the help of above equations give rise to

$$\int_0^\infty \left\{\alpha_1 + \alpha_2 A_1^{(1)}(s) + \alpha_3 A_2^{(1)}(s)\right\}\frac{\sin(sx)}{s}\,ds = 0, \qquad 0<x<a,\ b<x<\infty,$$

$$\int_0^\infty \left\{\beta_1 + \beta_2 A_1^{(1)}(s) + \beta_3 A_2^{(1)}(s)\right\}\frac{\cos(sx)}{s}\,ds = 0, \qquad 0<x<a,\ b<x<\infty.$$

Now setting

$$\alpha_1 + \alpha_2 A_1^{(1)}(s) + \alpha_3 A_2^{(1)}(s) = \int_a^b f_1(t)\cos(st)\,dt,$$

$$\beta_1 + \beta_2 A_1^{(1)}(s) + \beta_3 A_2^{(1)}(s) = \int_a^b f_2(t)\sin(st)\,dt,$$

where

$$\alpha_1 = \left(\frac{k^{(2)}(1+\eta^{(2)})\sqrt{\mu_1^{(2)}}}{2(\sqrt{\mu_2^{(2)}} - \sqrt{\mu_1^{(2)}})(1+k_1^{(2)})} \left(\frac{\sqrt{\mu_2^{(2)}}}{K^{(2)}} \right) + \frac{C_{66}^{(1)}}{C_{66}^{(2)}} \frac{k^{(1)}(1+\eta^{(1)})}{2K^{(1)}} \frac{\sqrt{\mu_1^{(2)}}(\sqrt{\mu_{22}^{(2)}} - K^{(1)})}{(1+k_1^{(2)})(\sqrt{\mu_2^{(2)}} - \sqrt{\mu_1^{(2)}})} \right)$$

$$- \left(\frac{k^{(2)}(1+\eta^{(2)})\sqrt{\mu_2^{(2)}}}{2(\sqrt{\mu_1^{(2)}} - \sqrt{\mu_2^{(2)}})(1+k_2^{(2)})} \left(\frac{\sqrt{\mu_1^{(2)}}}{K^{(2)}} \right) + \frac{C_{66}^{(1)}}{C_{66}^{(2)}} \frac{k^{(1)}(1+\eta^{(1)})}{2K^{(1)}} \frac{\sqrt{\mu_2^{(2)}}(\sqrt{\mu_{21}^{(2)}} - K^{(1)})}{(1+k_2^{(2)})(\sqrt{\mu_1^{(2)}} - \sqrt{\mu_2^{(2)}})} \right),$$

$$\alpha_2 = \left(\frac{\sqrt{\mu_1^{(2)}}(1+k_1^{(1)})(\sqrt{\mu_2^{(2)}} - \sqrt{\mu_1^{(1)}})}{\sqrt{\mu_1^{(1)}}(1+k_1^{(2)})(\sqrt{\mu_2^{(2)}} - \sqrt{\mu_1^{(2)}})} - \frac{\sqrt{\mu_2^{(2)}}(1+k_1^{(1)})(\sqrt{\mu_1^{(2)}} - \sqrt{\mu_1^{(1)}})}{\sqrt{\mu_1^{(1)}}(1+k_2^{(2)})(\sqrt{\mu_1^{(2)}} - \sqrt{\mu_2^{(2)}})} \right),$$

$$\alpha_3 = \left(\frac{\sqrt{\mu_1^{(2)}}(1+k_2^{(1)})(\sqrt{\mu_2^{(2)}} - \sqrt{\mu_2^{(1)}})}{\sqrt{\mu_2^{(1)}}(1+k_1^{(2)})(\sqrt{\mu_2^{(2)}} - \sqrt{\mu_1^{(2)}})} - \frac{\sqrt{\mu_2^{(2)}}(1+k_2^{(1)})(\sqrt{\mu_1^{(2)}} - \sqrt{\mu_2^{(1)}})}{\sqrt{\mu_2^{(1)}}(1+k_2^{(2)})(\sqrt{\mu_1^{(2)}} - \sqrt{\mu_2^{(2)}})} \right),$$

$$\beta_1 = \left(\frac{k^{(1)}\eta^{(1)}}{2K^{(1)}} - \frac{k^{(2)}\eta^{(2)}}{2K^{(2)}} \right),$$

$$\beta_2 = \left(\frac{k_1^{(2)}}{\sqrt{\mu_1^{(2)}}} \frac{\sqrt{\mu_1^{(2)}}(1+k_1^{(1)})(\sqrt{\mu_2^{(2)}} - \sqrt{\mu_1^{(1)}})}{\sqrt{\mu_1^{(1)}}(1+k_1^{(2)})(\sqrt{\mu_2^{(2)}} - \sqrt{\mu_1^{(2)}})} + \frac{k_2^{(2)}}{\sqrt{\mu_2^{(2)}}} \frac{\sqrt{\mu_2^{(2)}}(1+k_1^{(1)})(\sqrt{\mu_1^{(2)}} - \sqrt{\mu_1^{(1)}})}{\sqrt{\mu_1^{(1)}}(1+k_2^{(2)})(\sqrt{\mu_1^{(2)}} - \sqrt{\mu_2^{(2)}})} \right),$$

$$\beta_3 = \left(\frac{k_1^{(2)}}{\sqrt{\mu_1^{(2)}}} \frac{\sqrt{\mu_1^{(2)}}(1+k_2^{(1)})(\sqrt{\mu_2^{(2)}} - \sqrt{\mu_2^{(1)}})}{\sqrt{\mu_2^{(1)}}(1+k_1^{(2)})(\sqrt{\mu_2^{(2)}} - \sqrt{\mu_1^{(2)}})} + \frac{k_2^{(2)}}{\sqrt{\mu_2^{(2)}}} \frac{\sqrt{\mu_2^{(2)}}(1+k_2^{(1)})(\sqrt{\mu_1^{(2)}} - \sqrt{\mu_2^{(1)}})}{\sqrt{\mu_2^{(1)}}(1+k_2^{(2)})(\sqrt{\mu_1^{(2)}} - \sqrt{\mu_2^{(2)}})} \right)$$

and after lengthy process of mathematical manipulations, boundary conditions (4.14) and (4.15) finally lead to the following singular integral equations

$$a_1 f_1(x) + \frac{2}{\pi} \int_a^b \frac{f_2(t)}{(t-x)} dt = -\frac{2}{\pi} p_1(x), \qquad a \le |x| \le b, \tag{4.31}$$

$$c_1 f_2(x) + \frac{2}{\pi d_1} \int_a^b \frac{f_1(t)}{(t-x)} dt = -\frac{2}{\pi} p_2(x) - \frac{2c}{\pi x}, \quad a \le |x| \le b, \tag{4.32}$$

where

$$a_1 = \frac{2}{\pi} C_{66}^{(1)} \left[(1+k_1^{(1)}) \left(\frac{\beta_3}{\beta_3\alpha_2 - \alpha_3\beta_2} \right) + (1+k_2^{(1)}) \left(\frac{\beta_2}{\beta_2\alpha_3 - \alpha_2\beta_3} \right) \right],$$

$$\frac{1}{b_1}=\frac{2}{\pi}C_{66}^{(1)}\left[(1+k_1^{(1)})\left(\frac{\alpha_3}{\beta_3\alpha_2-\alpha_3\beta_2}\right)+(1+k_2^{(1)})\left(\frac{\alpha_2}{\beta_2\alpha_3-\alpha_2\beta_3}\right)\right],$$

$$c_1=\frac{2}{\pi}C_{66}^{(1)}\left[\frac{(1+k_1^{(1)})}{\sqrt{\mu_1^{(1)}}}\left(\frac{\alpha_3}{\beta_3\alpha_2-\alpha_3\beta_2}\right)+\frac{(1+k_2^{(1)})}{\sqrt{\mu_2^{(1)}}}\left(\frac{\alpha_2}{\beta_2\alpha_3-\alpha_2\beta_3}\right)\right],$$

$$\frac{1}{d_1}=\frac{2}{\pi}C_{66}^{(1)}\left[\frac{(1+k_1^{(1)})}{\sqrt{\mu_1^{(1)}}}\left(\frac{\beta_3}{\beta_3\alpha_2-\alpha_3\beta_2}\right)+\frac{(1+k_2^{(1)})}{\sqrt{\mu_2^{(1)}}}\left(\frac{\beta_2}{\beta_2\alpha_3-\alpha_2\beta_3}\right)\right],$$

$$c=\left[\frac{(1+k_1^{(1)})}{\sqrt{\mu_1^{(1)}}}\left(\frac{\alpha_3\beta_1-\alpha_1\beta_3}{\beta_3\alpha_2-\alpha_3\beta_2}\right)+\frac{(1+k_2^{(1)})}{\sqrt{\mu_2^{(1)}}}\left(\frac{\alpha_2\beta_1-\alpha_1\beta_2}{\beta_2\alpha_3-\alpha_2\beta_3}\right)+\frac{(1+\eta^{(1)})}{2}\frac{k^{(1)}}{K^{(1)}}\right]. \qquad (4.33)$$

Equations (4.31) and (4.32) are reduced to the following singular integral equations for the determination of unknown functions $f_i(x)$.

$$\phi_k(x)+\frac{1}{\pi\, i\,\varepsilon_k\, r_k}\int_a^b\frac{\phi_k(t)}{(t-x)}dt=-g_k(x)-\frac{2\,i\,c}{\pi\, r_k\; x},\quad a\le|x|\le b, \qquad (4.34)$$

where

$$\phi_k(x)=\sqrt{a_1b_1}\,f_1(x)+ir_k\sqrt{c_1d_1}\,f_2(x),\quad k=1,2,$$

$$\varepsilon=\sqrt{a_1b_1c_1d_1},\;\; r_k=(-1)^{k+1},\qquad k=1,2,$$

$$g_k(x)=\frac{2}{\pi}[\sqrt{b_1/a_1}\,p_1(x)+r_k\sqrt{d_1/c_1}\,p_2(x)],\qquad k=1,2,$$

and $f_i(x)$ are satisfying the compatibility conditions $\int_a^b f_i(t)dt=0,\quad i=1,2.$

The solution of above integral equations in (4.34) may be assumed as

$$\phi_k(x)=\omega_k(x)\sum_{n=0}^{\infty}c_{kn}P_n^{(\alpha_k,\beta_k)}(x),\qquad k=1,2, \qquad (4.35)$$

where $\omega_k(x)=(1-x)^{\alpha_k}(1+x)^{\beta_k}$,

$$\alpha_k = -\frac{1}{2} + i\omega_k, \quad \beta_k = -\frac{1}{2} - i\omega_k, \quad \omega_k = r_k \omega \text{ and } \omega = \frac{1}{2\pi}\ln\left|\frac{1+\varepsilon}{1-\varepsilon}\right|,$$

with c_{kn} are unknown constants. Now using equation (4.33), we get $\int_a^b \phi_i(t)dt = 0,\ i = 1, 2,$ which implies $c_{k0} = 0, \quad k = 1, 2.$

From equations (4.34) and (4.35), we get

$$\omega_k(x) \sum_{n=1}^{\infty} c_{kn}\, P_n^{(\alpha_k \beta_k)}(x) + \frac{2}{\pi\, i\ \varepsilon\, r_k} \int_a^b \frac{\omega_k(t) \sum_{n=0}^{\infty} c_{kn} P_n^{(\alpha_k, \beta_k)}(t)}{(t-x)} dt = -g_k(x) - \frac{2\,i\,c}{\pi\, r_k}\sqrt{\frac{d_1}{c_1}}\frac{1}{x}. \tag{4.36}$$

Multiplying the above equation by $P_j^{(\alpha_k,\beta_k)}(x)$ and integrating from -1 to 1, we get

$$c_{l\,j}\theta_j^{(\alpha_k,\beta_k)} + \frac{2}{\pi\, i\, \varepsilon_k r_k}\sum_{n=1}^{\infty} c_{kn}\, L_{njk} = -F_{kj} - \frac{2\,i\,c}{\pi\, r_k}\sqrt{\frac{d_1}{c_1}}\int_{-1}^{1}\frac{P_j^{(\alpha_k,\beta_k)}(x)}{x}dx, \tag{4.37}$$

where $\theta_j^{(\alpha_k,\beta_k)} = \left(\frac{2^{\alpha_k+\beta_k+1}}{2\,j + \alpha_k + \beta_k + 1}\frac{\Gamma(j+\alpha_k+1)\Gamma(j+\beta_k+1)}{\Gamma(j+\alpha_k+\beta_k+1)\ j!}\right),$

$$L_{njk} = \int_{-1}^{1} P_j^{(\alpha_k,\beta_k)}(x)\int_a^b \frac{\omega_k(t)P_n^{(\alpha_k,\beta_k)}(t)}{(t-x)}dt\,dx,$$

$$F_{kj} = \int_{-1}^{1} g_k(x)P_j^{(\alpha_k,\beta_k)}(x)dx, \ k = 1,\ 2, \quad j = 1,\ 2,$$

and the principal value of $\int_{-1}^{1}\frac{dx}{x}$ is considered as zero.

Finally the stress intensity factors at the crack tips $x = a$ and $x = b$ are calculated as

$$\sqrt{b_1/a_1}\ \ K_I{}^a + ir_k\sqrt{d_1/c_1}\ K_{II}{}^a = \lim_{x\to a-}(x-a)^{-\alpha_k}(x+a)^{-\beta_k}[\sqrt{b_1/a_1}\sigma_{yy}^{(1)}(x,0) + ir_k\sqrt{d_1/c_1}\sigma_{xy}^{(1)}(x,0)]$$

$$= \frac{(-1)^{\alpha_k}\pi\, a}{2}\sum_{n=1}^{\infty} c_{k\,n}P_n^{(\alpha_k,\beta_k)}(1), \quad k = 1,\ 2. \tag{4.38}$$

$$\sqrt{b_1/a_1}\;K_I^{\,b}+ir_k\sqrt{d_1/c_1}\;K_{II}^{\,b}=\lim_{x\to b+}(x-b)^{-\alpha_k}(x+b)^{-\beta_k}[\sqrt{b_1/a_1}\sigma_{yy}^{(1)}(x,0)+ir_k\sqrt{d_1/c_1}\sigma_{xy}^{(1)}(x,0)]$$

$$=\frac{(-1)^{\alpha_k}\pi b}{2}\sum_{n=1}^{\infty}c_{kn}P_n^{(\alpha_k,\beta_k)}(1),\quad k=1,\,2. \tag{4.39}$$

The expression of the crack energy is given by

$$W=\int_a^b p_1(x)[v^{(1)}(x,0)-v^{(2)}(x,0)]\,dx. \tag{4.40}$$

4.4 Results and discussion

In this section, the numerical computations have been done to find physical quantities viz., stress intensity factors and crack energy for two collinear cracks situated at the interface of two pairs of orthotropic materials with first one as α-Uranium and Epoxy Boron, and the second one as Beryllium and Epoxy Boron. In each case first type of material is taken as half plane-1 and second type of material as half plane-2. During computations crack length is considered as $b=1$ and $a=0.1(0.1)0.9$ and also the loadings are considered as $p_1(x)=p$, $p_2(x)=0$. The ratios of the stress temperature coefficients $\beta_y^{(1)}/\beta_x^{(1)}$ and $\beta_y^{(2)}/\beta_x^{(2)}$ are taken as 0.67 and 0.5 respectively for first pair of materials, and 0.7 and 0.5 respectively for second pair of materials. The elastic constants of the orthotropic material α-Uranium have been taken as $C_{11}=21.47\times10^6\,psi$ $(148.03\;GPa)$, $C_{12}=4.65\times10^6\,psi$ $(32.06\;GPa)$, $C_{22}=19.36\times10^6\,psi$ $(133.48\;GPa)$, $C_{66}=7.43\times10^6\,psi$ $(51.22\;GPa)$ (Das and Patra (2005)). The elastic constants of the other considered orthotropic material Boron-Epoxy has been taken as $C_{11}=30.3\times10^6\,psi$ $(208.91\,GPa)$, $C_{12}=3.78\times10^6\,psi$ $(26.06\;GPa)$, $C_{22}=4.04\times10^6\,psi$

$(27.85\ GPa)$, $C_{66} = 1.13\times10^{6}\ psi$ $(7.79\ GPa)$ (Sih and Chen (1978)), and those of orthotropic material Beryllium are taken as $C_{12} = 8.88\times10^{6}\ psi$ $(61.22\ GPa)$, $C_{22} = 36.49\times10^{6}\ psi$ $(251.58\ GPa)$, $C_{66} = 11.24\times10^{6}\ psi$ $(77.4\ GPa)$ (Das and Patra (2005)). For first and second pair of materials, the stress intensity factors at the tip $x = a$ are described through Fig. 4.2 and Fig. 4.3 respectively for different values of *a/b*, whereas the physical quantities at the tip $x = b$ for both the pair of materials are depicted through Figs. 4.4 - 4.5 for various *a/b*. The numerical values of crack energies for two pair of materials are shown through Figs. 4.6 - 4.7 for different values of *a/b*.

It is seen from Figs. 4.2 that as the length of the crack decreases, both K_I^a and K_{II}^a decrease. Same nature is followed for second pair of materials (Fig. 4.3) with only difference is that the values of stress intensity factors change as it completely depends on material constants.

As the lengths of the cracks decrease (Figs. 4.4 - 4.5) i.e., cracks separation distance increases, then K_I^b decreases, K_{II}^b increases under thermo-mechanical loading for both the pair of materials. This shows that there is a least possibility of crack propagation at $x = b$, even when the tips of the cracks come very close to each other. The decreases of Mode II stress intensity factor justifies that as the distance between two cracks decreases, the effect of their propagation tendency in sliding mode will be decreased.

The nature of behavior of crack energy for first pair of materials is same as the second pair of materials with the difference is that in first case the nature of the decrease is very fast as compared to the gradually decrease of the second case.

In the numerical computation it is also given special emphasis to determine other physical quantity crack energy W to determine the energy required by the crack per unit increase in area. Figs. 4.6 and 4.7 shows that crack energy increases with increase of crack length. The increment of crack energy represents that as crack advances then plastic zone size becomes large due to which more energy will be required for the crack propagation after attaining its critical value.

It is seen from the Figs. 4.2 - 4.5 that first pair of materials can sustain more stress intensity compared to second pair of materials without fracture and it is also justified from Figs. 4.6 - 4.7 that for the first pair of materials the crack energy is higher compared to second pair of materials due to formation of large plastic zone at the crack tips with increase of crack length.

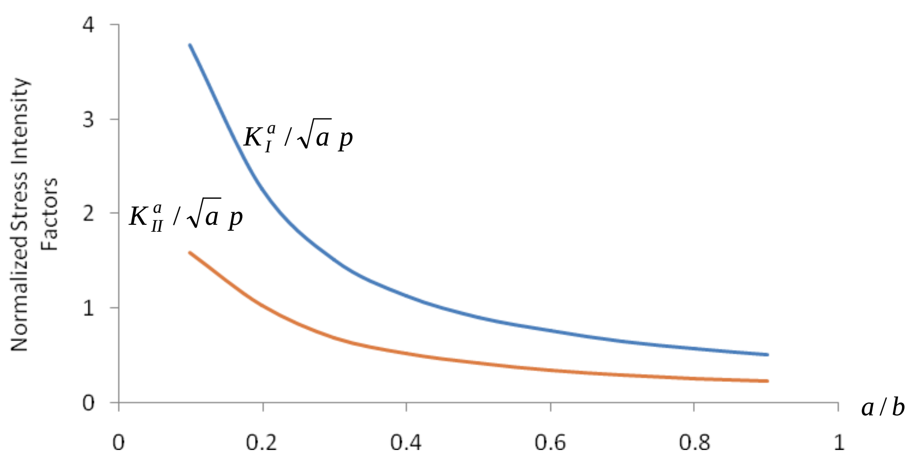

Fig. 4.2 Plots of $K_I^a/\sqrt{a}\,p$ and $K_{II}^a/\sqrt{a}\,p$ vs. a/*b* for first pair of materials

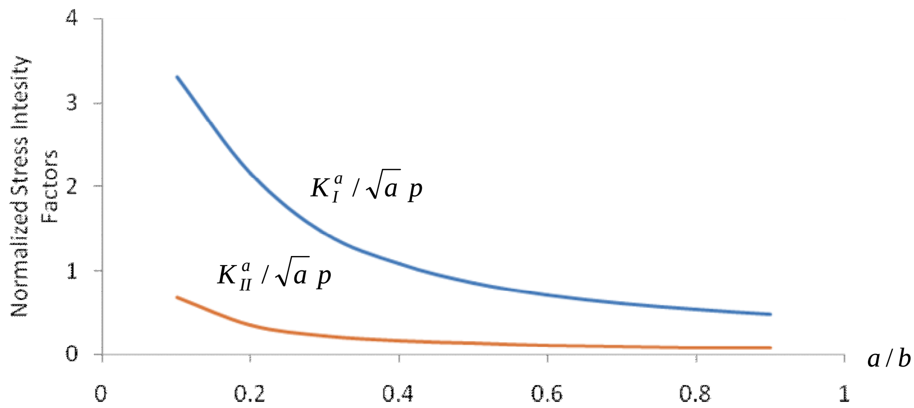

Fig. 4.3 Plots of $K_I^a / \sqrt{a}\ p$ and $K_{II}^a / \sqrt{a}\ p$ vs. a / b for second pair of materials

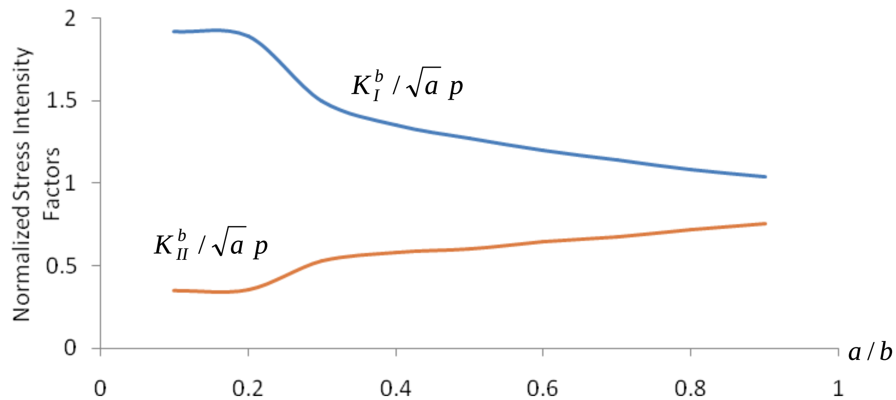

Fig. 4.4 Plots of $K_I^b / \sqrt{a}\ p$ and $K_{II}^b / \sqrt{a}\ p$ vs. a / b for first pair of materials

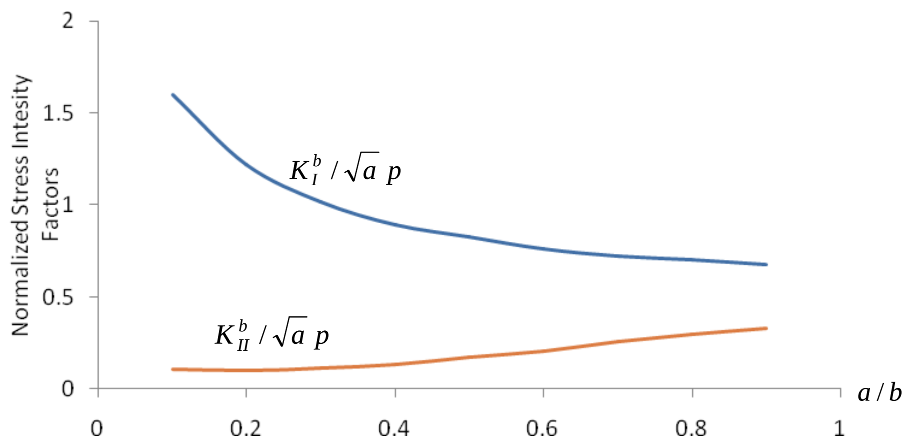

Fig. 4.5 Plots of $K_I^b / \sqrt{a}\ p$ and $K_{II}^b / \sqrt{a}\ p$ vs. a / b for second pair of materials

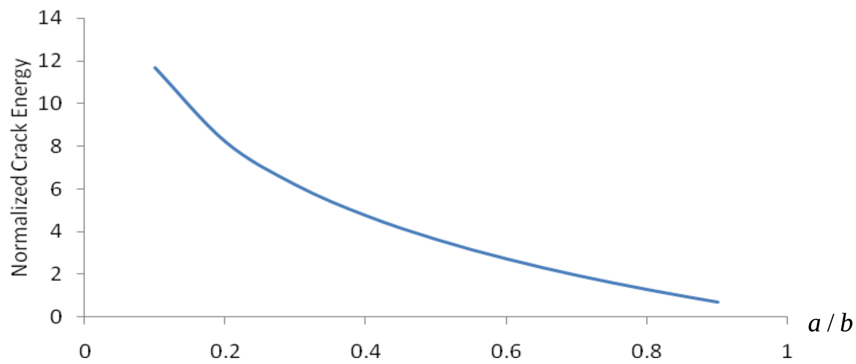

Fig. 4.6 Plot of $W/a\,p$ vs. a/b for first pair of materials

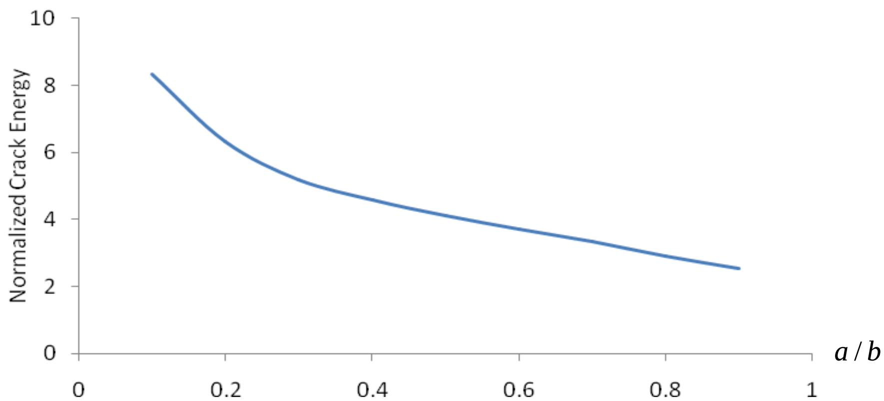

Fig. 4.7 Plot of $W/a\,p$ vs. a/b for second pair of materials

4.5 Conclusion

In the present chapter four important goals are achieved. The first one is the investigation of a pair of collinear Griffith cracks at the interface of two orthotropic media under thermo-mechanical loading. Second one is finding the analytical form of the stress intensity factors at the vicinity of the crack tips. Third one is the successful presentation of variations of the stress intensity factors with crack separation distance. Fourth one is the increase of crack energy due to increase of length of the cracks showing the possibility of the formation of large plastic zone at the vicinity of the crack tip.